EUROPEAN ORGANIZATION FOR NUCLEAR RESEARCH

Proposal to the ISOLDE and Neutron Time-of-Flight Committee

Evolution of $N = 50$ shell and neutron single-particle states towards ^{78}Ni: ^{79}Zn$(d,p)^{80}$Zn

January 5, 2022

E. Sahin[1], G. de Angelis[2], H.C. Berg[3], V. Bildstein[4], N. Erduran[5], R. Gernhaeuser[6], D. Gjestvang[1], S. Golenev[6], A. Görgen[1], M. Guttormsen[1], K. Hadyńska-Klęk[7], A. Illana[8], V. W. Ingeberg[1], P. Jones[9], A.C.Larsen[1], K.C.W. Li[1], K.L. Malatji[9], M. Markova[1], A. Matta[10], J. Pakarinen[8], W. Paulsen[1], L.G. Pedersen[1], L.Pellegri[9], F. Pogliano[1], S. Siem[1], T. Tornyi[1], M. Yalcinkaya[11], M. Wiedeking[9], P. Reiter[12], K. Arnswald[12], M. Droste[12], H. Hess[12], H. Kleis[12], A. Spyrou[3], S. Liddick[3]

[1] *University of Oslo, Oslo, Norway*
[2] *INFN Laboratori Nazionali di Legnaro, Italy*
[3] *Michigan State University, East Lansing, Michigan, USA*
[4] *Department of Physics, University of Guelph, Guelph, Ontario, Canada*
[5] *Sabahattin Zaim University, Istanbul, Turkey*
[6] *Physics Department, Technical University of Munich, D-85748 Garching, Germany*
[7] *Heavy Ion Laboratory, University of Warsaw, Poland*
[8] *Accelerator Laboratory, University of Jyävaskylä, Jyävaskylä, Finland. Helsinki Institute of Physics, Helsinki, Finland.*
[9] *iThemba LABS, South Africa*
[10] *Laboratoire de Physique Corpusculaire de Caen, 14050 CAEN CEDEX 4, France*
[11] *University of Istanbul, Department of Physics, Istanbul, Turkey*
[12] *Institut für Kernphysik, Universität zu Köln, Köln, Germany*

Spokespersons: E. Sahin eda.sahin@fys.uio.no
Contact person: Karl Johnston karl.johnston@cern.ch

Abstract: The aim of the present proposal is to explore neutron single-particle states in the neutron-rich ^{80}Zn nucleus via the one-neutron pickup reaction in inverse kinematics, ^{79}Zn$(d,p)^{80}$Zn. The high-lying neutron core excited states are not known so far and will be populated and identified through measurements of the angular distribution of proton recoils of this direct one-step reaction. The ^{79}Zn beam at an energy of 5 MeV/A will be impinging on a deuterated-polyethylene target. Emitted protons and γ rays de-exciting the states in the residual nucleus will be detected using the T-REX + MINIBALL setup, respectively. If the statistics allow, the same reaction and setup will be used to study the statistical properties of the quasi-continuum states and to constrain the ^{79}Zn(n,γ) cross section for the first time in the proposed experiment. In order to increase the statistics of the γ rays at higher energies, 6 LaBr$_3$ detectors from the University of Oslo will be installed.

Requested shifts: 21 shifts for the ^{79}Zn beam plus 3 shifts to optimize the production and purification of the beam.
Installation: MINIBALL + T-REX + 6 LaBr$_3$ detectors from Oslo

1 Motivation

1.1 Evolution of the $N = 50$ shell gap

The main objective of the proposal is to explore the evolution of the neutron $N = 50$ shell gap towards ^{78}Ni. The evolution of the $N = 50$ shell closure comprises the nuclei from $Z = 40$ (^{90}Zr) to $Z = 28$ (^{78}Ni) along the $N = 50$ isotonic chain. The present study proposes to determine the size of the gap and changes in the effective single-particle energies via neutron excitations above the $N = 50$ shell gap, which is between $\nu 2d_{5/2}$ and $\nu 1g_{9/2}$ orbitals. Identification of the excited states due to these $1p - 1h$ intruder configurations in $N = 50$ isotones gives direct knowledge of the evolution of the $N = 50$ gap and the single-particle orbitals [1].

The calculated wave functions for the particle-hole ($np-nh$, n=1,2,3,4 at most) excitations above the $N = 50$ shell gap show the presence of a significant component of $1p - 1h$ excitation with the ($\nu 1g_{9/2}^{-1} \otimes \nu 2d_{5/2}$) configuration [2]. Similarly, large scale shell-model (LSSM) calculations using pf-shell orbitals for protons and f$_{5/2}$, p, g$_{9/2}$, and d$_{5/2}$ orbitals for neutrons concluded that neutron excitations above the $N = 50$ gap are important in order to understand changes in the neutron effective single-particle energies [3]. The calculations predicted the shell gap to reach a minimum at $Z = 32$ and increase towards $Z = 28$ as expected. The resulting states arising from the ($\nu 1g_{9/2}^{-1} \otimes \nu 2d_{5/2}^1$) configuration form a multiplet with J^π=2$^+$, 3$^+$, 4$^+$, 5$^+$, 6$^+$, 7$^+$.
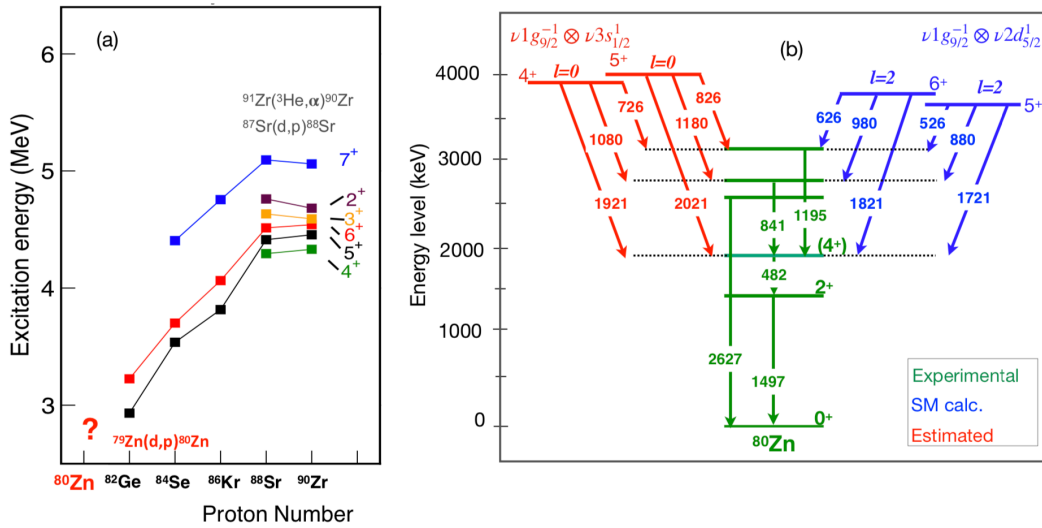

Figure 1: (a) Evolution of the $1p - 1h$ excited states in the even-even $N = 50$ isotones. (b) Experimental level scheme of ^{80}Zn from [9] (green). States at 3.7 and 3.8 MeV (blue) are predictions from the SM calculations [3]. The estimated $3s_{1/2}$ states at 3.9 and 4 MeV (red) are also given See the text for the details.

Figure 1a shows the experimentally identified $1p - 1h$ states in the even $N = 50$ iso-tones. A complete identification of these multiplets along the $N = 50$ isotonic chain has been done for $^{90}_{40}$Zr and $^{88}_{38}$Sr so far via one-neutron pickup reactions, ^{91}Zr(^{3}He,α)^{90}Zr and ^{87}Sr(d,p)^{88}Sr, respectively [4, 5]. Starting from $^{86}_{36}$Kr, the multiplet was only partially identified [6]. The $^{82}_{32}$Ge nucleus is the last member of the chain where only the 5$^+$ and

6^+ states could be identified as members of the $1p - 1h$ multiplet, when compared to the LSSM predictions [2].

($\nu 1g_{9/2}^{-1} \otimes \nu 2d_{5/2}^1$) states: None of the states of the $\nu 1g_{9/2}^{-1} \otimes \nu 2d_{5/2}^1$ multiplet in ^{80}Zn is known at present. States belonging to the multiplet will be populated and can be identified by requiring an angular momentum transfer of $l = 2$. This is possible since the $9/2^+$ ground state of ^{79}Zn is dominated by the $(g_{9/2}^{-1})$ neutron-hole configuration [7].

The first excited 2^+ state at 1497 keV in ^{80}Zn is known from a Coulomb excitation experiment performed at ISOLDE [8]. Other low-lying states are populated via a nucleon knockout reaction up to around 3.5 MeV at RIKEN [9]. However, none of the higher-lying states belonging to the $1p - 1h$ multiplet could be identified. Figure 1b shows the level scheme of ^{80}Zn adopted from Ref. [9]. In order to estimate the cross sections of the final states via the (d,p) channel, the Shell model predictions from Ref. [3] are used. The calculations predicted the 5^+ and 6^+ states at around 3.7 and 3.8 MeV, respectively, with a dominant particle hole configuration where one neutron is excited to the $2d_{5/2}$ orbital.

($\nu 1g_{9/2}^{-1} \otimes \nu 3s_{1/2}^1$) states: There will be other spin multiplets with 4^+ and 5^+ from the transfer of a ($l = 0$) neutron into the $3s_{1/2}$ orbit., i.e. the $\nu 1g_{9/2}^{-1} \otimes \nu 3s_{1/2}^1$ configuration. In the case of ^{80}Zn, the energy difference between the two orbitals $2d_{5/2}$ and $3s_{1/2}$ is expected to be less than the one in ^{88}Sr ($Z = 38$) primarily due to the lowering of the $3s_{1/2}$ state towards ^{80}Zn ($Z = 30$). In fact, the energy difference between the $1/2^+$ g.s. and $5/2^+$ states in the neutron-rich $N = 51$ isotones was experimentally shown to decrease from 1.2 MeV in ^{91}Zr to 0.28 MeV in ^{83}Ge [10]. Therefore, in order to estimate the reaction cross sections, the states of the $\nu 1g_{9/2}^{-1} \otimes \nu 2d_{5/2}^1$ are considered to lie 200 keV above the $\nu 1g_{9/2}^{-1} \otimes \nu 2d_{5/2}^1$ multiplets, denoted as "estimated" in Fig. 1b. Note that there are no SM calculations for these states which would require a larger model space.

($\nu 1g_{9/2}^{-2} \otimes \nu 3s_{1/2}^2$) states: A $1/2^+$ isomeric state at 1.05(15)MeV has been observed in ^{79}Zn [7]. Later the magnetic moment measurement at ISOLDE reported this state to have a wave function dominated by a $1p - 2h$ neutron excitation across the $N = 50$ shell gap, i.e. $\pi 3s_{1/2} \otimes 1g_{9/2}^{-2}$ configuration [11]. In the present reaction, adding one neutron to the $3s_{1/2}$ orbital can populate $2p - 2h$ neutron excitations above $1g_{9/2}$, resulting in a 0^+ intruder state. The observation of such a 0^+ state in the proposed experiment would give experimental evidence for shape coexistence in ^{80}Zn, only two protons away from ^{78}Ni.

DWBA calculations and single-particle cross sections: DWBA calculations have been performed for the $l = 0$ and $l = 2$ states using the code FRESCO [12]. Angular distribution of protons emitted in the reaction are calculated using the deuteron optical model parametrization in Ref. [13] and the proton parameters from [14]. Figure 2a shows the excited states used in the calculations. The states with the 4^+ and 5^+ spins from the ($\nu 1g_{9/2}^{-1} \otimes \nu 3s_{1/2}^1$) interaction are given at 3.9 and 4 MeV as guess values, mentioned above. For the ($\nu 1g_{9/2}^{-1} \otimes \nu 2d_{5/2}^1$) multiplet, $2^+, 3^+, 4^+, 5^+, 6^+$, and 7^+ states at the excitation energies of 4.0, 3.9, 3.6, 3.7, 3.8, and 4.3 MeV, respectively, are considered. Note that while the excitation energies for 5^+ and 6^+ are taken from Ref. [3], the energies for the other spin members are scaled down using the energy values obtained for ^{90}Zr and ^{88}Sr given in Fig.1a. For the $l = 2$ states, the single-particle cross sections increase from ~ 10

3

to ∼30 mb with increasing spin while from ∼25 to ∼35 mb for the $l = 0$ states, shown in Fig. 2b. Figure 2c shows the calculated differential cross sections as a function of proton scattering angle in the center of mass for both multiplets. The obtained single-particle and differential cross sections as well as gamma-decay patterns given in Fig.1b are used as input in the Geant4 simulations in the next section. A spectroscopic factor of 1 is assumed in the DWBA calculations.
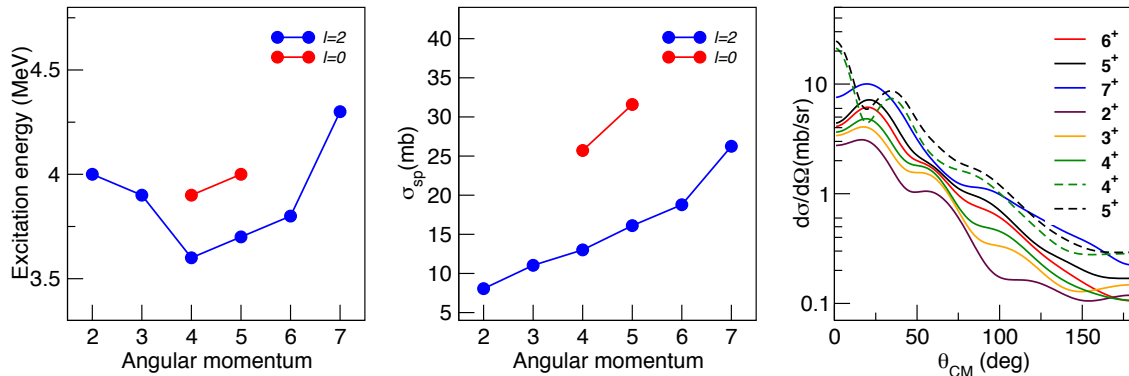

Figure 2: (a) Excitation energies and (b) single-particle cross sections for the $2d_{5/2}$ (blue) and $3s_{1/2}$ states (red). (c) Differential cross sections for the $2d_{5/2}$ states (solid lines) and for the two $3s_{1/2}$ states (dashed lines)

2 Experiment

We propose to measure the neutron particle-hole states of ^{80}Zn via single-neutron transfer reaction ^{79}Zn (d, p) ^{80}Zn in inverse kinematics. The ^{79}Zn beam will be post-accelerated to an energy of 395 MeV (5 MeV/A), impinging on a 1 mg/cm^2 deuterated-polyethylene CD$_2$ target. The target thickness is chosen to provide sufficient statistics for the population of the states of interest and results in 1 MeV of an energy resolution for the proton detection which is rather poor. Nevertheless, a thinner target would not provide a significant improvement as the excited states are expected to lie rather close in energy in the present case. The particle-γ (pγ) coincidence technique will be used for the identification of the excited states whether they are d ($l = 2$) or s ($l = 0$) type. It has been already employed successfully by previous studies at REX-ISOLDE [15]. Furthermore, p$\gamma\gamma$ coincidence analysis will help build the level scheme. A production yield of 5×10^5 ions/μA for ^{79}Zn has been previously achieved using a UC$_x$ target and laser ionized using RILIS [16] at the target position. Assuming an average 1.6μA of proton beam current and a 5% transmission efficiency to the MINIBALL beam line, the beam intensity on the MINIBALL target has been estimated to be about 4×10^4 pps. The experimental setup will consist of the T-REX silicon-detector array [17] coupled to the MINIBALL γ-ray spectrometer [18]. This setup permits the detection of the emitted protons in coincidence with the γ rays de-excited from the residual nucleus.

Geant4 simulations have been performed using the *nptool* simulation package [19]. In addition to the detector geometries, the single-particle and differential cross sections given in Fig.2b and c are implemented in the simulations. Figure 3a shows the energy versus laboratory angle, θ_{lab}, for the scattered protons detected in the T-REX particle array resulting in an acceptance of 60% for the particle detection. With a 1 mg/cm^2 target

thickness and 4×10^4 pps of a beam intensity, an absolute photo-peak efficiency of 6% at 1 MeV for MINIBALL, and an average cross section of 20 mb for the $2d_{5/2}$ and 28 mb for the $3s_{1/2}$ states:

- 1400 particle-γ rays and 150 particle-$\gamma\gamma$ coincidence events on average for the $2d_{5/2}$ states from 2^+ to 7^+
- 1750 particle-γ rays and 250 particle-$\gamma\gamma$ coincidence events for each $3s_{1/2}$ state (i.e. 4^+ and 5^+) are expected after **7 days of beam time**.

The requested beam time is necessary in order to obtain sufficient $\gamma\gamma$ coincidence data (for level scheme construction) and both proton and γ-ray angular distributions for a clear identification.
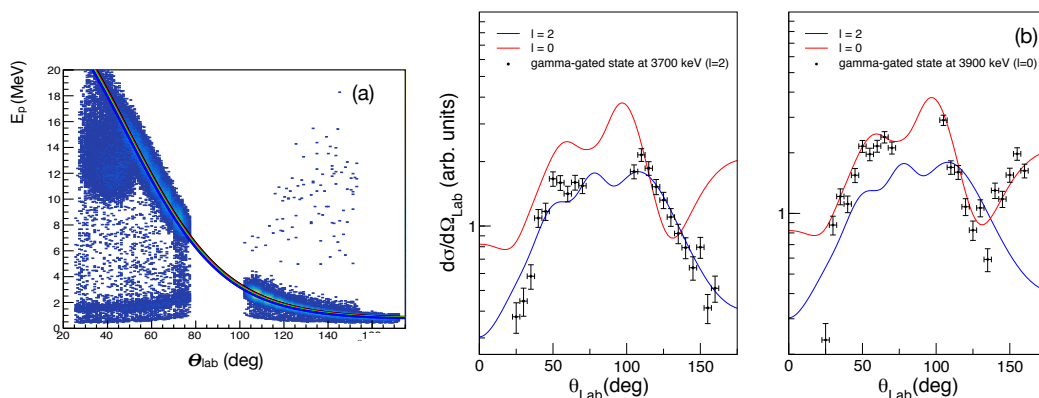

Figure 3: (a) Simulated energy of the scattered protons as a function of theta angle in the laboratory reference frame. (b) Simulated gamma-gated differential cross sections for the states at 3.7 ($l = 2$) and 3.9 MeV ($l = 0$). The DWBA calculations for $l = 2$ and $l = 0$ are included for comparison in both cases. Simulations take into account both T-REX and MINIBALL efficiencies. Number of events are obtained for 7 days of beam time.

The simulated γ-gated differential cross sections after 7 days of beam time are shown in Figure 3b for the 5^+ ($\nu 1g_{9/2}^{-1}\otimes\nu 2d_{5/2}^1$) and 4^+ states ($\nu 1g_{9/2}^{-1}\otimes\nu 3s_{1/2}^1$). The sum of the γ gates at 526, 880, and 1721 keV is used for the 3700-keV state while the γ gates of 726, 1080, and 1921 keV are summed for the 3900-keV state given in Fig. 1b. The comparison of these distributions to the DWBA estimations indicates that the $l = 2$ and $l = 0$ angular momentum transfers as well as the spin of the expected states can be identified once the proton scattering distributions are selected via proper γ-ray tagging.

2.0.1 ^{79}Zn(n,γ) cross section and r-process around $A = 80$ mass region

The ^{79}Zn(d,pγ) reaction will populate the excited states up to the neutron-separation energy (S_n= 6.2 MeV) thus, suitable for measuring the (n,γ) cross section of the ^{79}Zn seed nucleus as will be explained below. This is particularly important for the sensitivity studies of the neutron capture reaction in the context of the weak r-process that forms primarily the A $\sim$ 80 r-process peak [20]. At high excitation energy in the region of the neutron binding energy, where the excited states form a quasi-continuum, the nucleus is described by statistical properties such as the nuclear level density (NLD) and gamma-ray strength function (gSF). Here, the NLD is the total number of states accessible in a given excitation energy and the gSF is the probability that a γ ray of a certain energy will be emitted from an excited nucleus. The Oslo Method [21] will be used to extract these

quantities. In the Oslo method, an iterative procedure is applied to extract the primary gamma rays from a given excitation energy bin by a weighted subtraction of gamma rays from lower excitation energies. (Fig. 4a). The resulting matrix of primary gamma rays as a function of excitation energy (Fig. 4b) can be factorized into the NLD and gSF [22]. The experimental NLD and gSF, including their uncertainties, can then be used in Hauser-Feshbach calculations to calculate the (n,γ) cross section. This technique provides more realistic predictions compared to calculations purely based on theory and on generic NLD and gSF models, as has been demonstrated for several cases [23, 24, 25, 26]. This is illustrated in Fig. 4c, where different NLD and gSF models were used in Hauser-Feshbach calculations with the TALYS code [29], with an estimate of the expected uncertainties. The theoretical σ(n,γ) rates in the figure are calculated using 6 different NLD and 5
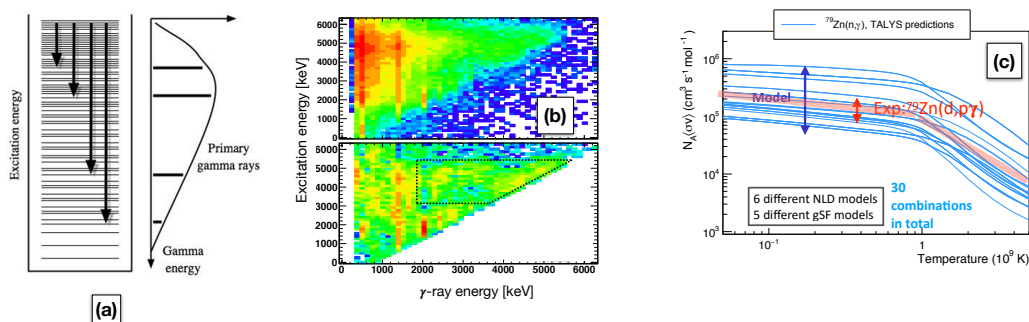

Figure 4: (a) illustration of primary gamma rays emitted from a highly excited state; (b) raw gamma-ray spectra for many excitation-energy bins (top) and primary gamma rays (bottom) from the ^{86}Kr(d,pγ)^{87}Kr reaction [22]; (c) calculated neutron-capture reaction rates (blue lines) using different NLD and gSF models. The red band illustrates the expected constrained rate when applying the data from this proposal [30].

different gSF models (30 combinations in total), resulting in a wide range of reaction rates on the y-axis [30]. The presented proposal aims at constraining the uncertainty for the (n,γ) reaction rate by an order of magnitude similar to the reduction obtained earlier for ^{70}Ni [27, 21]. This will be possible in the present experiment where a similar number of pγ events ($\sim$72000 pγ in Ref. [28]) in the first generation matrix is expected. In total $\sim$75000 pγ events for ^{80}Zn are estimated after comparing the conditions of the previously performed Oslo method experiment (IS559: ^{66}Ni(d,p)^{67}Ni) [31]. To increase the efficiency of detecting the higher energy γ rays for the Oslo method we propose to add 6 large volume LaBr$_3$ detectors. The details will be given in the PAC discussions.

Remarks on the particle-detectors: The present experiment is proposed to use the TREX-MINIBALL setup for reaching the objectives described. In case that an experimental campaign using the existing T-REX array is not feasible, HI-TREX, presently being developed at REX-(HIE)ISOLDE [32], will be used. This option would delay the scheduling of the experiment, but, on the other hand, improve the expected results since it is optimized for an effective investigation of transfer reactions. The newly developed, highly segmented silicon detector and the accompanying ASIC based electronics will improve aspects like electronics noise, background rate, pile-up and especially the kinematical reconstruction capabilities for close lying excited states.

Summary of requested shifts: 21 shifts for the ^{79}Zn beam plus 3 shifts to optimize the production and purification of the beam.

6

References

[1] O. Sorlin and M.-G. Porquet, Prog. Part. Nucl. Phys. **61**, 602 (2008).

[2] E. Sahin *et al.*, Nucl. Phys. A **893**, 1-12 (2012).

[3] K. Sieja and F. Nowacki, Phys. Rev. C **85** 051301(R) (2012).

[4] C. R. Bingham *et al.*, Phys. Rev. C **2** 2297 (1970).

[5] K. K. Seth *et al.*, Phys. Rev. C **10** 1928 (1974).

[6] J. Prevost *et al.*, Eur. Phys. J. A **22**, 391 (2004) and references therein.

[7] R.Orlandi *et al.*, Phys. Letts. B **740**, 298 (2015).

[8] J. Van de Walle *et al.*, Phys. Rev. Lett. **99**, 142501 (2007).

[9] Y. Shiga *et al.*, Phys. Rev. C **93** 024320 (2016).

[10] J.S. Thomas *et al.*, Phys. Rev. C **76** 044302 (2007).

[11] X. F. Yang *et al.*, PRL **116**, 182502 (2016).

[12] I. J. Thompson, Comput. Phys. Rep. **7**, 167 (1988).

[13] J. M. Lohr and W. Haeberli, Nucl. Phys. A **232**, 381(1974).

[14] R. L. Varner, W. J. Thompson,T. L. McAbee, E. J. Ludwig,T. B. Clegg, Phys. Rep. **201**,57 (1991).

[15] J. Diriken *et al.*, Phys. Rev. C **91**, 054321 (2015).

[16] B. A. Marsh *et al.*, Hyperfine Interactions Vol. 196, 129 (2010).

[17] V. Bildstein *et al.*, Eur. Phy. Journ A. **48**, 85 (2012).

[18] N. Warr *et al.*, Eur. Phys. J. A**49** (2013) 40.

[19] A Matta *et al.* J. Phys. G: Nucl. Part. Phys. **43** 045113 (2016).

[20] R. Surman *et al.*, AIP Advances 4, 041008 (2014).

[21] A. C. Larsen *et al.*, Phys. Rev. C **83**, 034315 (2011) and references therein.

[22] V. W. Ingeberg, Master thesis 2016: http://urn.nb.no/URN:NBN:no-56444.

[23] A. Spyrou et al., Phys. Rev. Lett. **113**, 232502 (2014).

[24] B. V. Kheswa, et al., Phys. Lett. B **744**, 268 (2015).

[25] A.C. Larsen et al., Phys. Rev. C **93**, 045810 (2016).

[26] K.L. Malatji et al., Phys. Lett. B **791**, 403 (2019).

[27] S.N. Liddick *et al.*, PRL **116**, 242502 (2016).

[28] A. C. Larsen *et al.*, Phys. Rev. C **97**, 054329 (2018).

[29] A. Koning, S. Hilaire, M. Duijvestijn, TALYS: Nuclear Reaction Simulator. URL: https://tendl.web.psi.ch/tendl 2019/talys.html.

[30] A. C. Larsen, Private communication.

[31] S. Siem, M. Wiedeking et al., IS559 experiment.

[32] C. Berner et al., Nucl. Inst. and Meth. in Physics Research, A **987**, 164827 (2021) .

Appendix

DESCRIPTION OF THE PROPOSED EXPERIMENT
The experimental setup comprises: (*name the fixed-ISOLDE installations, as well as flexible elements of the experiment*)

Part of the	Availability	Design and manufacturing
(MINIBALL + T-REX/HI-TREX)	⊠ Existing	⊠ To be used without any modification
[6 LaBr$_3$(Ce) detectors	□ Existing	□ To be used without any modification □ To be modified
	⊠ New	□ Standard equipment supplied by a manufacturer □ CERN/collaboration responsible for the design and/or manufacturing
[Part 2 of experiment/ equipment]	□ Existing	□ To be used without any modification □ To be modified
	□ New	□ Standard equipment supplied by a manufacturer □ CERN/collaboration responsible for the design and/or manufacturing
[insert lines if needed]		

HAZARDS GENERATED BY THE EXPERIMENT (if using fixed installation:) Hazards named in the document relevant for the fixed [MINIBALL + only CD, MINIBALL + T-REX] installation.

Additional hazards:

Hazards	[Part 1 of experiment/ equipment]	[Part 2 of experiment/ equipment]	[Part 3 of experiment/ equipment]
Thermodynamic and fluidic			
Pressure	[pressure][Bar], [volume][l]		
Vacuum			
Temperature	[temperature] [K]		
Heat transfer			
Thermal properties of materials			
Cryogenic fluid	[fluid], [pressure][Bar], [volume][l]		
Electrical and electromagnetic			
Electricity	[voltage] [V], [current][A]		
Static electricity			

Magnetic field	[magnetic field] [T]		
Batteries	☐		
Capacitors	☐		
Ionizing radiation			
Target material [material]	CD2		
Beam particle type (e, p, ions, etc)	^{79}Zn		
Beam intensity	$4x10^4$ pps		
Beam energy	5 MeV/u		
Cooling liquids	liquid N_2		
Gases	[gas]		
Calibration sources:	☐		
• Open source	☐		
• Sealed source	☐ Standard γ-ray source for MINIBALL [ISO standard]		
• Isotope			
• Activity			
Use of activated material:			
• Description	☐		
• Dose rate on contact and in 10 cm distance	[dose][mSV]		
• Isotope			
• Activity			
Non-ionizing radiation			
Laser			
UV light			
Microwaves (300MHz-30 GHz)			
Radiofrequency (1-300 MHz)			
Chemical			
Toxic	[chemical agent], [quantity]		
Harmful	[chem. agent], [quant.]		
CMR (carcinogens, mutagens and substances toxic to reproduction)	[chem. agent], [quant.]		
Corrosive	[chem. agent], [quant.]		
Irritant	[chem. agent], [quant.]		
Flammable	[chem. agent], [quant.]		
Oxidizing	[chem. agent], [quant.]		
Explosiveness	[chem. agent], [quant.]		

Asphyxiant	[chem. agent], [quant.]		
Dangerous for the environment	[chem. agent], [quant.]		
Mechanical			
Physical impact or mechanical energy (moving parts)	[location]		
Mechanical properties (Sharp, rough, slippery)	[location]		
Vibration	[location]		
Vehicles and Means of Transport	[location]		
Noise			
Frequency	[frequency],[Hz]		
Intensity			
Physical			
Confined spaces	[location]		
High workplaces	[location]		
Access to high workplaces	[location]		
Obstructions in passageways	[location]		
Manual handling	[location]		
Poor ergonomics	[location]		

Hazard identification:

Average electrical power requirements (excluding fixed ISOLDE-installation mentioned above): [make a rough estimate of the total power consumption of the additional equipment used in the experiment]: ... kW